Journal of Molecular Liquids 348 (2022) 118051

Contents lists available at ScienceDirect

Journal of Molecular Liquids

journal homepage: www.elsevier.com/locate/molliq

Open chain pseudopeptides as hydrogelators with reversible and dynamic responsiveness to pH, temperature and sonication as vehicles for controlled drug delivery

Adriana Valls, M. Isabel Burguete, Laura Kuret, Belén Altava *, Santiago V. Luis *

Departamento de Química Inorgánica y Orgánica, Universitat Jaume I, Av. de Vicent Sos Baynat, s/n 12071, Castellón, Spain

ARTICLE INFO

Article history:
Received 19 May 2021
Revised 29 October 2021
Accepted 7 November 2021
Available online 11 November 2021

Keywords:
Controlled release
Pseudopeptides
Hydrogels
Self-assembly
Transdermal delivery

ABSTRACT

A new family of open chain-pseudopeptidic compounds displaying a pendant carboxylic group have been prepared with excellent yields. Their self-assembly has been studied under different conditions and in different media. Some of the compounds obtained have revealed to act as very efficient hydrogelators at low concentrations (CGC 1 mg mL^{-1}). The resulting hydrogels show some interesting properties, including a high thermal stability, with the hydrogels maintaining their structure at temperatures above 65 °C, and their reversible dynamic sol–gel behavior being responsive to thermal and sonochemical inputs and to changes in the basic/acidic properties of the medium. Preliminary studies for controlled drug delivery have been carried out using a Franz Cell and employing a skin pig membrane, confirming that these Low Molecular Weight Gelators (LMWGs) can be appropriate vehicles for the controlled transdermal delivery of small-molecule drugs.

1. Introduction

Self-assembly refers to the process of spontaneous organization of biotic and synthetic molecules into higher order structures involving supramolecular interactions [1–4]. In this context, gelators are generally defined as chemical species that, in a given solvent, self-assemble to form crosslinked networks able to immobilize solvent molecules, giving place to the formation of a gel. Although a variety of natural and synthetic polymers are known to act as efficient gelators, low-molecular weight gelators (LMWGs) present some interesting features. These include their well-defined molecular weights, their easy modification, or the accessibility of a large abundance of structural functionalities [5–8].

As in other instances, self-assembly of LMWGs to form gels rely on supramolecular forces like hydrogen bonding, electrostatic, π-π or hydrophobic interactions [5–14]. Hydrogels, those formed in aqueous systems, are of special biological relevance and display a wide variety of potential applications like tissue engineering [15–16], controlled drug delivery [17–19], or even nanoscale electronics [20]. Some of them behave as stimuli-responsive materials [21–24], with properties, including their formation and disruption, controlled by stimuli ranging from changes in temperature, which is the more obvious input, to pH changes [18,25–27], irradiation at a variety of wavelengths [28–30], or through the presence of a variety of substances including biomolecules [31–32].

Gels with tunable, reversible, and dynamic gel-sol transitions become especially desirable for applications in fields like smart materials and on-demand release [33–35]. Thus, for instance, polypeptide based thermosensitive hydrogels have been reported to provide targeted and controlled delivery of drugs to tumor microenvironments [36], while a variety of injectable hydrogels have been used to encapsulate substrates *in vivo* [37–39]. Furthermore, transdermal drug delivery systems based on hydrogels have been widely used [40].

In this context, hydrogelators based on amino acids, their derivatives and peptides are very attractive because of the modular character of the amino acid fragments, their natural origin and, accordingly, their potential for biocompatibility and biodegradability [41–44].

Minimalistic pseudopeptides, combining structural elements from amino acids and simple abiotic fragments, are attractive for this purpose [45]. In this regard, carbamate protected amino acids and derivatives have been reported as very effective hydrogelators [46–48], while C_2-symmetry pseudopeptidic compounds displaying apolar spacers have shown a remarkable organogelating behavior [49], with the presence of urea fragments increasing significantly the stability of the resulting gels [50]. Thus, tripodal

* Corresponding author.
E-mail addresses: altava@uji.es (B. Altava), luiss@uji.es (S.V. Luis).

https://doi.org/10.1016/j.molliq.2021.118051
0167-7322/

trisurea pseudopeptidic organogelators were able to gel essential oils from natural flavors and fragrances and modulate their controlled release [51]. Including polar functionalities in the spacer, like secondary amino groups, in these C_2-symmetry pseudopeptides led to hydrogelators with self-assembly properties controlled by pH changes [52].

Taking this into account, here we report on the preparation of open chain C_2-symmetry pseudopeptides containing a carboxylic pendant group in the spacer that can be used to generate stable hydrogels possessing responsiveness to different stimuli, including temperature and pH, and are promising materials for transdermal controlled delivery of small-molecule drugs.

2. Materials and methods

2.1. Materials

Reagents and solvents were purchased from commercial suppliers and used without further purification. The C_2-symmetrical N-protected bis(amidoamines) **1** were prepared as previously described [22]. Deionized water was obtained from a MilliQ® equipment (Burlington, MA, USA).

2.2. ***Electron*** *microscopy*

Scanning Electron Microscopy was performed either in a LEO 440I or in a JEOL 7001F microscope with a digital camera. Samples were obtained by slow evaporation of a solution of the compound (5 mg mL^{-1}) directly onto the sample holder, and were conventionally coated previous to the measurement.

2.3. NMR ***spectroscopy***

NMR experiments were carried out on a Varian INOVA 500 spectrometer (500 MHz for ^1H and 125 MHz for ^{13}C) or on a Varian UNITY 400 (400 MHz for ^1H and 101 MHz for ^{13}C). Chemical shifts are reported in parts per million using the solvent residual peak as the reference.

2.4. Infrared ***spectroscopy***

ATR FT-IR spectra were acquired on a JASCO 6200 equipment having a MIRacle Single Reflection ATR Diamond/ZnSe accessory. Samples in solution, in the gel state or in solid state were directly deposited onto the ATR sample holder, and the FT-IR spectra were collected. The raw IR data were processed with the JASCO spectral manager software.

2.5. UV–vis ***spectroscopy***

UV–vis absorption measurements used a Hewlett-Packard 8453 spectrophotometer, having a controlled temperature system.

2.6. ***Preparation*** *of buffer solutions*

- *Phosphate buffers*: Buffers were prepared by dissolving the corresponding amount of KH_2PO_4 and K_2HPO_4 in 100 mL of miliQ® water. The pH was then adjusted with small additions of 1 M HCl and/or 1 M NaOH.
- *Acetate buffers*: Buffers were prepared using the corresponding amount of AcOH 10 mM and NaAcO 10 mM in miliQ® water. The pH was then adjusted with small additions of AcOH or NaAcO 10 mM.

2.7. ***Gelation*** *experiments*

In a typical experiment, a weighted amount of LMWG was mixed with 2 mL of the selected solvent in a 12 mL glass vial, ultrasonicated for 1 min and left resting at rt for 24 h. Gelation was defined when a homogeneous mixture was obtained exhibiting no gravitational flow upon inversion of the vial. For organic/water solvent mixtures, the LMWG was first dissolved in the corresponding amount of the organic solvent (DMSO or EtOH) and later miliQ® water or the appropriate aqueous buffer was added. Samples with clear gel formation can show some gel particles on the glass wall, these particles do not correspond to partly flowing gels but to the splashes produced during sonication.

2.8. ***Rheological*** *characterization*

The different gels were characterized using a controlled stress AR-2000 rheometer from TA Instruments. A Peltier holder with a plate geometry (60 mm diameter, 500 μm gap) was used for all samples. Frequency sweeps were performed in the angular frequency range 0.1–100 rad s^{-1} with the instrument in oscillatory mode at 25 °C. Strain sweeps were performed using a frequency of 1 rad s^{-1} in an amplitude sweep range of 0.01% – 80% with the instrument in oscillatory mode at 25 °C.

2.9. Release studies

The appropriate amounts of gelator and drug were weighted and mixed with the corresponding solvent mixture to obtain the desired gels as described before. The experiments were conducted in a Franz Diffusion Cell where the gel was formed *in situ* on the donor compartment cell. The acceptor compartment was filled with 5 mL of phosphate buffer (10 mM, pH = 7.3) maintaining a mild magnetic stirring, and the porcine skin was placed in the diffusion area. The system was closed to avoid solvent evaporation. The experiments were conducted in duplicate or triplicate, at 35 °C for up to 24 h. Aliquots (100 μL) from the acceptor compartment were taken at different times and evaluated using a Hewlett-Packard 8453 spectrophotometer (UV–vis spectroscopy) equipped with a control temperature system to determine the amount of caffeine or (*S*)-Naproxen released. For this purpose, the corresponding aliquot was diluted with 1 mL of phosphate buffer (10 mM, pH = 7.3).

2.10. Data ***analysis***

The cumulative amount (Q, μg/cm^2) of caffeine and (*S*)-Naproxen penetrating through an area of 1.3 cm^2 was plotted against time (t). The steady-state flux J_{SS} (g/cm^2h) was determined from the slope of the linear portion of the cumulative amount (Q μg/cm^2) versus time (t) plot.

The diffusion coefficients through the gel were calculated based on a non-steady-state diffusion model with the equation for the early-time being $M_t/M_o = 4(D_E{}^*(t\text{-}l)/h^2\ \pi)^{1/2}$ and the one for the late-time being: $M_t/M_o = 1 - 8/\ \pi\ ^2(\exp - \pi\ ^2D_L(t\text{-}l)/h^2)$, where M_t is the total amount of molecules released during the measurement, M_o is the total amount of molecules loaded on the hydrogel matrix, h represents the hydrogel thickness, t is the time of measurement, and D is the diffusion constant of the molecule,

In order to study the drug transport mechanisms from the hydrogels, the empirical equation used to analyze the Fickian and the non-Fickian release of drug is: $M_t/M_\infty = k(t\text{-}l)^n$, where, M_t/M_∞ is the fraction of drug released at time t, l is the lag time and n is a diffusional exponent indicating the mechanism of drug transport.

This equation can be used to analyze only the first 60% of release, regardless of geometric shapes.

Five diffusion models were considered to which the experimental data were fitted:

Higuchi equation: $M_t/M_\infty = k\ t^{1/2}$, where M_t/M_∞ is the fraction of drug released, k is a kinetic constant, and t is the release time.

Ritger–Peppas equation: $M_t/M_\infty = kt^n$, where M_t/M_∞ is the fraction of drug released, k is a kinetic constant, n represents the diffusional exponent indicating the mechanism of transport of drug, and t is the release time.

Peppas–Sahlin equation: $M_t/M_\infty = k_1\ t^n + k_2\ t^{2n}$, where M_t/M_∞ is the fraction of drug released, the first term of the equation represents the contribution of the Fickian diffusion, and the second term refers to the macromolecular relaxation contribution on the overall release mechanism.

Alfrey equation: $M_t/M_\infty = k_1\ t^{0.5} + k_2\ t$, described also by the Peppas–Sahlin equation, but with the exponent n fixed to 0.5.

Zero order equation: $M_t/M_\infty = kt$, where M_t/M_∞ is the fraction of drug released, k represents the constant for zero order release and t is the release time.

For cylindrical systems and when $0.45 < n < 0.89$, more than one mechanism controls the release; for $n < 0.45$ the Fickian diffusion controls the release and for $n \geq 1$ anomalous transport occurs. k is a kinetic constant (having units of t^{-n}) incorporating structural and geometric characteristics of the delivery system.

2.11. *General* synthesis for compounds 2a-c

The corresponding pseudopeptidic N-protected bis(aminoamide) precursor **1a-c** (4 mmoles), 4-(dimethylamino)pyridine (0.8 mmoles) and succinic anhydride (8 mmol) were dissolved in Et_3N-THF 1:1 (50 mL). The reaction mixture was stirred and heated at 70 °C for 24 h. The solvent was vacuum evaporated, the crude was dissolved in acidic water and extracted with CH_2Cl_2 (3x), the organic layer was washed with water and then dried with anhydrous $MgSO_4$. The organic solvent was vacuum evaporated and the white solid obtained purified by column chromatography (CH_2Cl_2:MeOH, 10:1).

2a. White solid. 70% Yield. m.p. = 114 °C, $[\alpha]_D^{25} = -6.24$ deg cm^3 g^{-1} dm^{-1} (c = 0.005 g cm^{-3}, CH_3OH). ^{1}H NMR (400 MHz, CD_3OD, δ): 7.42–7.21 (m, 10*H*), 5.16–5.03 (m, 4H), 3.89 (t, *J* = 9.3 Hz, 2H), 3.55–3.32 (m, 8H), 2.68–2.56 (m, 4H), 2.12–1.95 (m, 2H), 0.92 (dd, *J* = 10.6, 6.8 Hz, 12H); ESI$^+$, *m*/*z* (%): 670.7 [M + H]$^+$, 692.7 [M + Na]$^+$; 708.7 [M + K]$^+$. ESI$^-$, *m*/*z* (%): 668.7 [M – H]$^-$, 704.7 [M – H + 2H_2O]$^-$; ^{13}C NMR (126 MHz, CD_3OD, δ): 173.4, 173.1, 157.2, 136.8, 128.1, 127.6, 127.5, 66.4, 60.9, 45.0, 37.3, 37.1, 30.3, 28.9, 27.6, 18.4, 17.0; DEPT (101 MHz, $CDCl_3$, δ): 175.53, 174.66, 172.4, 171.9, 157.4, 156.5, 136.3, 136.1, 128.5, 128.2, 128.0, 67.3, 67.0, 60.2, 49.0, 45.7, 40.0, 38.6, 32.0, 31.0, 29.4, 27.9, 19.3, 17.8, 17.4; FT-IR (ATR) (cm^{-1}): 3290, 3202, 3105, 2968, 1709, 1648, 1528, 1237, 1022; Anal. Calcd. for $C_{34}H_{47}N_5O_9$. 1.5 H_2O: C, 58.2; H, 7.3; N, 10.0. found: C, 57.9, H, 6.9, N, 10.2.

2b. White solid, 85% yield. m.p. = 117 °C, $[\alpha]_D^{25} = -4.93$ deg cm^3 g^{-1} dm^{-1} (c = 0.005 g cm^{-3}, CH_3OH). ^{1}H-RMN (500 MHz, CD_3OD, δ): 7.27–7.41 (m, 10*H*), 5.03–5.18 (m, 4H), 3.94 (dd, *J* = 10.5, 7.2 Hz, 2H), 3.56–3.27 (m, 8H), 2.54–2.72 (m, 4H), 1.83 (s, 2H), 1.51 (s, 2H), 1.1–1.25 (m, 2H), 0.87–0.95 (m, 12H); ^{1}H NMR (500 MHz, $CDCl_3$, δ): 7.26 (s, 10*H*), 6.71 (s, NH), 5.79 (s, NH), 5.35 (s, NH), 5.20–4.85 (m, 4H), 4.19 – 3.86 (m, 3H), 3.67 (s, 2H), 3.29–3.10 (m, 3H), 2.94 (s, 1H), 2.78 (s, 2H), 2.51–2.43 (m, 1H), 2.24 (s, 1H), 1.85–1.57 (s, 3H), 1.38 (s, 2H), 1.18 (s, 1H), 1.00 (s, 2H), 0.80 (s, 12H); ESI$^+$, *m*/*z*(%): 698.8 [M + H]$^+$; 720.7 [M + Na]$^+$, 736.6 [M + K]$^+$; ESI$^-$, *m*/*z* (%): 696.8 [M−H]$^-$, 732.7 [M−H + 2H_2O]$^-$; ^{13}C NMR (101 MHz, $CDCl_3$, δ): 175.4, 174.9, 172.4, 171.7, 157.3, 156.4, 136.3, 136.0, 128.5, 128.15, 128.0, 67.3, 67.0, 59.6, 59.5, 49.2, 45.7, 40.3, 38.7, 37.3, 29.5, 27.9, 24.7, 24.51, 15.5, 11.5, 11.3; Anal. Calcd. for $C_{36}H_{51}N_5O_9 \cdot H_2O$: C, 60.4; H, 7.5; N, 9.8. found: C, 60.6, H, 7.2, N, 9.7.

2c. White solid, yield 59%. m.p. = 108 °C, $[\alpha]_D^{25} = -2.10$ deg cm^3 g^{-1} dm^{-1} (c = 0.008 g cm^{-3}, CH_3OH). ^{1}H-RMN (101 MHz, CD_3OD, δ): 7.37–7.14 (m, 20H), 5.20–4.90 (m, 4H), 4.42–4.25 (m, 2H), 3.50–3.25 (m, 8H), 3.25–3.03 (m, 2H), 2.96–2.75 (m, 2H), 2.65 (s, 4H); ESI$^+$ *m*/*z* (%): 766.7 [M + H]$^+$, 788.7 [M + Na]$^+$, 804.5 [M + K]$^+$; ESI$^-$ *m*/*z* (%): 764.6 [M – H]$^-$, 800.7 [M – H + 2H_2O]; ^{13}C-RMN (101 MHz, CD_3OD /$CDCl_3$, δ): 175.4, 173.4, 172.7, 172.5, 156.5, 136.7, 136.3, 129.1, 128.3, 127.9, 127.6, 126.7, 66.7, 56.4, 47.1, 45.2, 38.2, 37.7, 29.0, 27.6; DEPT (101 MHz, CD_3OD, δ): δ 173.5, 173.1, 172.9, 156.8, 137.3, 137.2, 128.9, 128.1, 127.5, 127.3, 126.4, 66.2, 45.1, 37.7, 37.4, 37.3, 28.7, 27.6.; IR (ATR) (cm^{-1}): 3313, 3282, 2952, 2361, 2338, 1731, 1690, 1652, 1532, 1452, 1429, 1383, 1287, 1260, 1241,1179, 1141, 1053; Anal. Calcd. for $C_{42}H_{47}N_5O_9$: C, 60.4; H, 6.3; N, 8.9, found: C, 60.0; H, 6.2; N, 9.1.

3. Results and discussion

3.1. *Synthesis* of pseudopeptidic compounds as LMWGs

The procedure for the synthesis of the C_2-symmetry pseudopeptides **2a-c** is shown in Scheme 1. Compounds **1a-c** were obtained following the previously reported general synthetic procedure [53]. The corresponding compound **1** was then reacted with succinic anhydride in THF : Et_3N (1:1) in the presence of 4-(dimethylamino)pyridine [54]. After acidification of the reaction crude, the desired compounds **2a-c** were obtained as white solids in good yields. The presence of the additional amide group and the carboxylic fragment were expected to increase the polarity of the spacer, with the acidic group allowing a pH regulated control of the properties.

Pseudopeptides **2a-c** were assayed as LMWGs. Supramolecular interactions leading to gel formation depend on structural factors, solvent type, pH, temperature and other variables [21–35,49,52]. Thus, their gelation properties were studied in water, in different aqueous mixtures, and in some organic solvents (Table S1).

None of the compounds formed gels (5.5 mg mL^{-1}) in traditional organic solvents like DMSO, EtOH or $CHCl_3$ (entries 5–7, Table S1) and only **2a** formed a hydrogel in pure water (entry 1, Table S1). However, **2a** and **2b** formed gels in hydroalcoholic mixtures and in water : DMSO mixtures (entries 2–4, Table S1). Finally, **2a** and **2b** also formed a gel in glycerol using a different protocol involving the heating of the mixture at 80 °C and a resting period of 42 h (entry 8, Table S1). The more stable hydrogels were formed by **2a**. These results highlight the importance of the hydrophobic / hydrophylic balance in the properties of LMWGs, with changes in the side chain of the amino acid providing important perturbations of their self-assembly behavior [55]. Hydrogels at this concentration (5.5 mg mL^{-1}) were slightly turbid while glycerol organogels were translucid (Fig. S13). Compound **2a** formed homogeneous and stable gels, for hydroalcoholic mixtures, in the 1–10 mg mL^{-1} concentration range, the hydrogels being translucid at the lower LMWG concentrations (Fig. S13b).

3.2. Thermal stability of the Hydrogels

Initial assessment of the stability of the hydrogels was carried out using the vial inversion test, and the same was used for a first analysis of their thermal stability [56]. Increasing the concentration of the gelator is known to increase the thermal stability of the gel, leading to higher T_{gel} (gelation temperature) values [57]. This was also observed for hydrogels formed by **2a** (Table 1) displaying T_{gel} values in H_2O/EtOH (9:1, v/v) ranging from 33 °C (2.5 mg mL^{-1}) to 65 °C (9.2 mg mL^{-1}). Above these temperatures

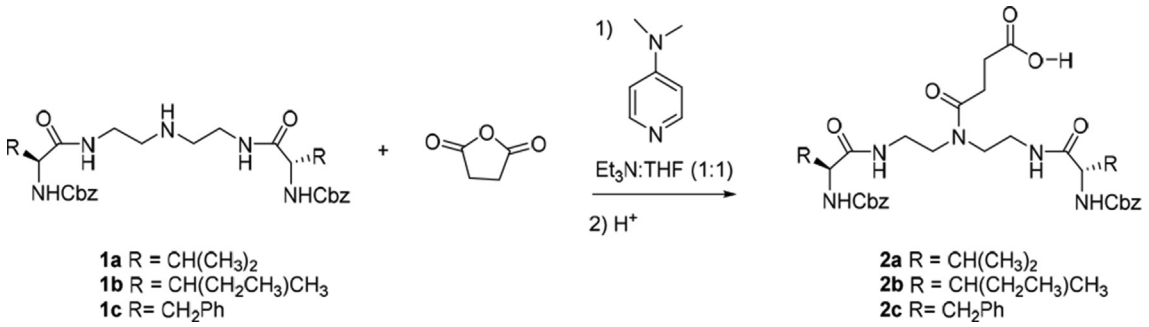

Scheme 1. Synthesis of LMWGs **2a-c.**

Table 1
Gelation properties of **2a** as a function of gelator content (mg mL^{-1}) in water/EtOH (9:1, v/v).

Entry	w/v (mg/mL)		T_{gel} (°C)[a]
1	1	wG	–
2	2.5	G	33
3	5.1	G	52
4	7.1	G	60
5	9.2	G	65
6	15	wG	–
7	5.5	G[b]	54
8	5.5	G[c]	60 (55[e])
9	5.5	G[d]	69

[a]Temperature of gel disassembly obtained with the inverted vial test. [b]H_2O/EtOH (8:2, v/v). [c]Glycerol as solvent. [d]H2O/DMSO (9:1, v/v) as solvent. [e]the value in brackets corresponds to **2b.**

the gel started to flow and changed to a solution. At concentrations of 1 and 15 mg mL^{-1}, **2a** formed weaker and / or less homogeneous hydrogels in the same medium, precluding an accurate determination of T_{gel} values. Higher LMWG concentrations were always accompanied by a slight increase in turbidity (Fig. S13b).

The EtOH content of the medium essentially did not affect the observed T_{gel} value (entries 3 and 7, Table 1), while the substitution of EtOH by DMSO produced an appreciable increase (entry 9, Table 1) for a *ca.* 5 mg mL^{-1} concentration of **2a**. The steric hindrance of the amino acid side chain seems to produce a decrease in the melting temperature of the organogel, associated to a less efficient self-assembly, as suggested by the comparison of T_{gel} values for **2a** and **2b** in glycerol (entry 8, Table 1).

The thermal stability of the hydrogels was also investigated by ^{1}H NMR spectroscopy (Fig. S14). The ^{1}H NMR spectra of the **2a**-hydrogel (5.5 mg mL^{-1}, D_2O/CD_3OD 9:1 v/v) in the 30–40 °C region did not allow to observe any signal assignable to **2a**, which is in agreement with a polymeric self-associated structure, while in the 50–60 °C region two broad peaks at 0.9 and 7.4 ppm start to be observed, corresponding to the methyl groups and the aromatic protons of **2a** as corresponds to the disassembly of the polymeric structure. The process is fully reversible, and the gel was completely reformed after 10 min when cooling back the sample to 30 °C.

Data presented in Table 1 allowed to assign a critical gelator concentration (CGC) of 1 mg/mL for **2a**. This is the minimum amount of gelator required to gelate 1 mL of solvent at a given temperature [19]. Such a value that compares well with those reported for other amino acid derived hydrogelators [58–59].

As hydrogel formation is based in establishing appropriate supramolecular interactions, both changes in the pH of the medium and the presence of additional species can be key in determining hydrogel properties. Thus, the effect of pH on hydrogel formation was studied using different buffers (phosphate or acetate 10 mM) to cover a wide range of pH values (from 4.0 to 8.0) and initially using 2.5 mg mL^{-1} of **2a**, a value relatively close to the CGC. Results obtained with the phosphate buffers can be of particular interest given the biological relevance of related media.

Results summarized in Table 2 indicate that hydrogel formation is always favored at pH < 7. While at pH = 6.7, a strong hydrogel was formed at a higher gelator content (6 mg mL^{-1}, entry 4, Table 2), [61] no gel was formed at pH = 7 (entries 5 and 6, Table 2). As the pKa of **2a** is predicted to be around 4–5 [53], an essentially full deprotonation of the carboxylic group in **2a** must take place at pH $\geq$ 7, which seems to inhibit the self-assembly, most likely by significantly increasing the solubility in water. The comparison of entries 1 and 2 in Table 2 shows that no significant effect was observed when reducing the concentration of the buffer.

In the same way, no appreciable differences were observed when the phosphate buffer was substituted by an acetate buffer (10 mM) allowing to study gel formation in the 4–6 pH region (entries 8–10, Table 2). At acidic pH values, gel disassembly temperatures (2.5 mg mL^{-1}) were essentially constant (44 ± 1 °C, vial inversion test) irrespective of the buffer nature and pH. An almost direct lineal correlation between the gelator content and $T_{gel,}$ was observed using the phosphate buffer at pH = 5.8 in H_2O/EtOH (9/1, v/v), as shown in Fig. 1.

Thus, the presence of the carboxylic group can provide a pH regulated behavior. In the case of related compounds containing an amine group in the spacer [52], the gels are formed in basic media, while, in the present case, the most stable gels are obtained in slightly acidic media. Thus, the easy preparation of both kinds of functionalities allows developing gels suitable either for acidic or basic conditions.

Gels from **2a** were stable for weeks under unchanged conditions. However, a change in the pH of the medium led to an almost instantaneous disassembly of the gel. It must be noted, also, that the chemical structure of the LMWG is very stable and is not expected to degrade under the assayed conditions. Under biological conditions, however, this kind of compounds have been observed to be degraded by proteases which represents an interesting feature in terms of their biodegradability [60].

UV–vis spectroscopy was also used to study T_{gel} was also studied by for a 2.5 mg mL^{-1} gelator content at pH 5.8 (phosphate buffer, 10 mM, (Fig. 2a), as the formation of the gel is accompanied by changes in the absorption at 600 nm, with the absorbance at this wavelength decreasing as the gel is broken. This allowed estimating a temperature of *ca.* 40 °C for the sol–gel transition [62]. The appreciable enhancement in thermal stability when the gelator content was increased to 5 mg mL^{-1} in the same medium (pH = 5.8) was also confirmed, with the disassembly of the gel taking place at *ca.* 60 °C (Fig. 2b).

It must be noted that when using H_2O/EtOH (9/1, v/v) with a 10 mM phosphate buffer (pH = 5.8) the CGC value determined was as low as 1 mg mL^{-1} (ESI, Table S2), though the resulting gel

Table 2
Gelation properties as a function of pH and buffer in water/EtOH (9:1) for **2a**[a].

Entry	pH	Buffer[b]	2a	T_{gel} (°C)[f]
1	5.8	KH_2PO_4/K_2HPO_4	G	43 (40)
2	5.8	KH_2PO_4/K_2HPO_4[c]	G	44
3	6.7	KH_2PO_4/K_2HPO_4	S	—
4	6.7	KH_2PO_4/K_2HPO_4[d]	G	55
5	7.0	KH_2PO_4/K_2HPO_4	S	–
6	7.0	KH_2PO_4/K_2HPO_4[e]	S	–
7	8.0	KH_2PO_4/K_2HPO_4	S	–
8	4.2	AcOH/AcONa	G	45
9	5.0	AcOH/AcONa	G	45
10	5.6	AcOH/AcONa	G	44

[a]2.5 mg/mL gelator unless otherwise stated. [b] 10 mM. [c] 5 mM. [d] 6 mg/mL gelator concentration. [e] 7 mg/mL gelator concentration. [f] Gel disassembly temperature obtained in the vial inversion test; in brackets T_{gel} obtained from UV experiments (600 nm).

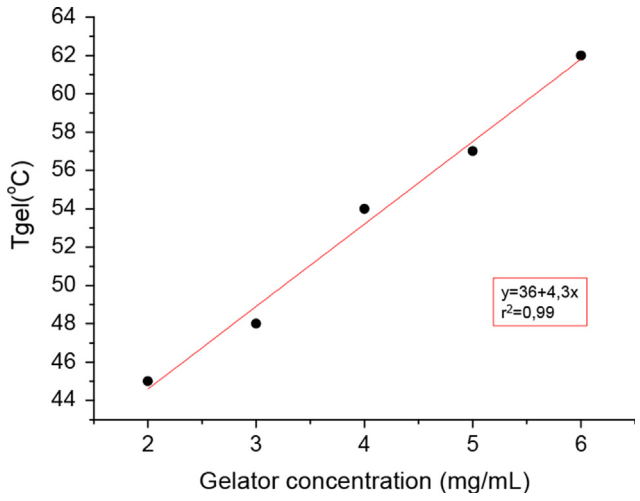

Fig. 1. Variation of the T_{gel} values as a function of the concentration of **2a** in H_2O : EtOH (9/1, v/v) using a 10 mM phosphate buffer (pH 5.8).

was a weak material, barely stable to vial inversion. Thus, the CGC values were very similar in pure H_2O/EtOH (9/1, v/v) and in the buffered medium, with the thermal stability of the gel formed in the buffered medium being always higher (entry 2, Table S2 and entry 2, Table 1).

SEM experiments provided additional insights into the microstructure of the self-assemblies formed by **2a** and **2b**. SEM images for the dried gels obtained from H_2O/EtOH (9:1, v/v) allowed to observe the presence of a well-defined interpenetrated network of regular nanofibers displaying diameters of *ca.* 35 nm (Fig. 3b for **2a** and S18a for **2b**).). It is worth mentioning that although **2a** is fully soluble in EtOH in the concentrations considered here, solvent evaporation also allowed to observe a tendency to form small nanofibrils (*ca.* 25 nm diameter, Fig. 3a) visible on rather amorphous regions [63–64]. In the presence of phosphate buffer (H_2O/EtOH, 9:1, v/v; pH = 5.8, gel formation), bundles of fibers exhibiting diameters higher than 1 μm can be observed (Fig. 3d for **2a**). In this last case, SEM pictures can be more complex to interpret, as the gelator and the buffer are at almost the same concentration, but control experiments in the absence of the gelator afforded SEM images with very different patterns (Fig. S19).

3.3. ^1H NMR and FT-IR spectroscopic studies

To obtain information on the supramolecular interactions present in these systems, a series of ^1H NMR and FT-IR experiments were carried out. In this regard, the comparison of the ^1H NMR spectra of **2a** (4 mM) in CD_3OD and $CDCl_3$ is illustrative. As shown in Fig. S14, in CD_3OD the aliphatic region of the spectrum displays a relatively simple set of signals confirming the presence of a C_2-symmetry and a high conformational flexibility. However, in $CDCl_3$ the spectrum indicates a complete loss of the C_2-symmetry with the observation, for instance, of two different signals for the proton at the stereogenic center (H_f) and for the signal of the methine of the isopropyl group (H_g). More relevant, even, is the observation of the loss of equivalence for the two protons of different methylene groups and amide and carbamate N-H signals (Fig. S4). This

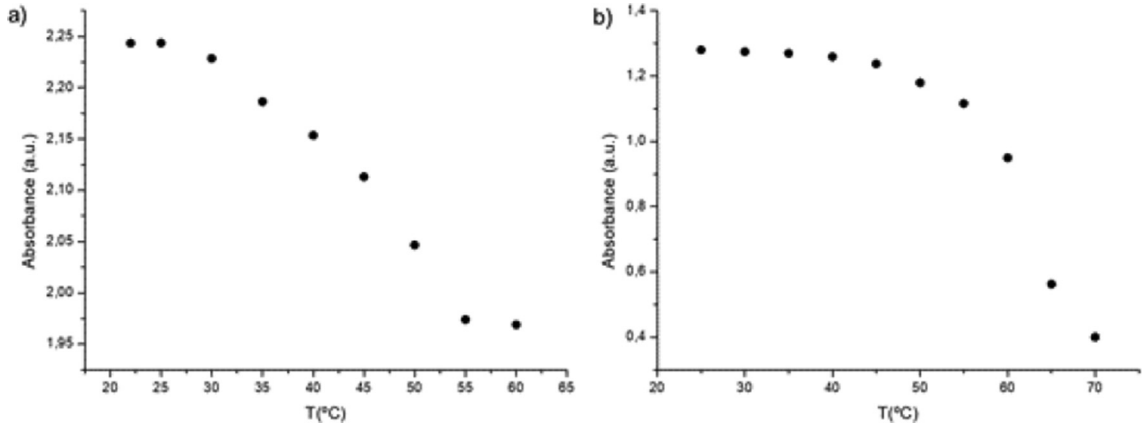

Fig. 2. UV absorption at 600 nm at different temperatures for **2a** at a) 2.5 mg mL^{-1} gelator content in phosphate buffer 10 mM (pH 5.8)/EtOH (9/1, v/v); b) 5 mg mL^{-1} gelator content in the same medium.

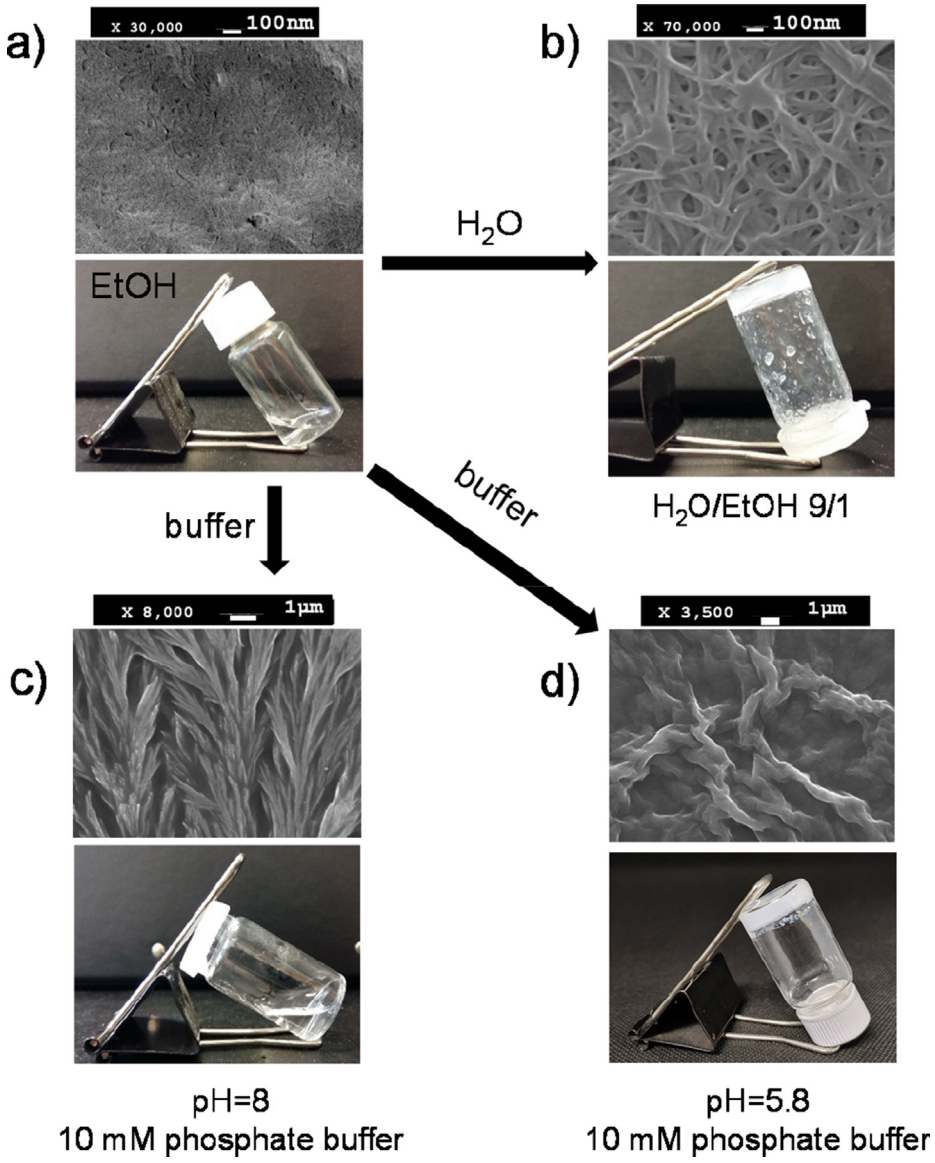

Fig. 3. a) Vial pictures (bottom) and SEM images of the corresponding dried solids (top) for the EtOH solution of **2a.** b) The gel formed in H_2O/EtOH (9:1, v/v, 5 mg mL^{-1} in **2a**). c) The sol formed in H_2O/EtOH (9:1, v/v, 5 mg mL^{-1} in **2a**) using a 10 mM phosphate buffer at pH = 8. d) The gel formed in H_2O/EtOH (9:1, v/v, 5 mg mL^{-1} in **2a**) using a 10 mM phosphate buffer at pH = 5.8.

suggests the prevalence of rigid conformations associated to the participation of intramolecular hydrogen bonding interactions that could be associated to the cis/trans isomerization of the Cbz carbamate bond or to the interaction of the central arm with one of the pseudopeptidic fragments. The use of a polar protic solvent like CD_3OD precludes the formation of such intramolecular hydrogen bonds (ESI, Fig. S15a). When aggregation studies were run in $CDCl_3$ (from 30 to 2 mM) some chemical shift changes with concentration were observed (ESI, Fig. S15b) particularly relevant for the amide and carbamate N-H signals. Organogels are not formed in such non-protic organic solvents at the low concentrations of relevance, but some nanofibers can be observed by SEM upon drying a solution from $CHCl_3$ (ESI, Fig. S18b).

The formation of gels in water / alcohol mixtures is accompanied by minor changes in the chemical shifts of the signals for **2a** and, more significantly, by a general broadening and lack of resolution of the signal with an important decrease in their intensity. A weak gel was obtained using a 5 mg mL^{-1} of **2a** in D_2O/CD_3OD 7:3 v/v in the NMR tube. After adding 2 equivalents of NaOH, the ^1H NMR signal for the methylene group next to the carboxyl group (H_d) shifts slightly to higher fields, indicating the formation of the carboxylate group, and, simultaneously, the intensity of all the signals increase as corresponds to the growth in the percentage of molecules present in solution and not in the polymeric self-assemblies (ESI, Fig. S16).

The comparison between the IR spectra of **2a** samples in the crystalline state and in the xerogel obtained by drying the hydrogel highlights the rather different assemblies present in both states (Fig. S17a). In the fibrillar hydrogel structure, both C = O_{st} bands shift to lower wavenumbers. Significant changes are also observed in the position and intensity of the bands corresponding to amide III and C-O_{st} for the carboxyl and carbamate groups (1200–1300 cm^{-1}). This indicates the presence of important differences between both samples in terms of hydrogen bonding and conformational preferences [65–66]. The FT-IR spectra for the hydrogel, after subtraction the contribution of the solvent (Fig. S17b), also contained relevant differences with the xerogel, in particular in the C-O_{st} regions and in the intensity of the bands in the amide II

region. This can be attributed to the additional hydrogen bonding with the protic solvents of molecules in the outer shell of the fibrils. The study by FT-IR of the hydrogels at different temperatures also confirms the disassembly taking place at around 60 °C, in agreement with results from other techniques.

3.4. Rheological measurements

Mechanical properties of the hydrogels were studied through rheological measurements [67]. A typical LMWG presents a storage and a loss modulus (Ǵ and Ǵ, respectively), which are frequency independent, and will break at relatively low strain [67]. Moreover, from the rheological data, the effect of temperature and concentration can be seen directly. It is generally expected that increasing the concentration will lead to the formation of more self-assembled structures with a higher cross-linking. Therefore, increasing the concentration of LMWG should lead to an increase in the rheological properties.

Fig. 4 displays the rheological results for the gel obtained from **2a** (5 mg mL^{-1}), using phosphate buffer (pH 5.8, 10 mM)/DMSO (9/1 v/v) as the medium. The storage modulus (G') of the gel was much higher than the loss modulus (G") over the whole range of frequency swept, which is characteristic of gelation. The strain sweep measurement (inset in Fig. 4a) showed that both the storage and loss moduli of the gel stayed constant up to 1% strain, the so-called linear viscoelastic region (LVER); beyond this region, the storage modulus began to plunge down as the strain increased. No significant differences were observed when EtOH was used as co-solvent instead of DMF for hydrogels containing 5 and 2.5 mg mL^{-1} of gelator (ESI, Fig. S20). Moreover, the storage modulus (G') obtained for the gel at 5 mg mL^{-1} was higher than the one for the gel at 2.5 mg mL^{-1}. However, the organogel obtained in glycerol displayed lower Ǵ and Ǵ parameters than the corresponding hydrogels and at frequencies higher than 50 Hz the organogel properties were lost (Fig. S21). Furthermore, the rheological properties of the gels were studied as a function of temperature, though for the hydrogel formed in phosphate buffer (pH 5.8, 10 mM)/EtOH (9/1 v/v) no reliable data could be obtained, due to EtOH evaporation during the measurement. Fig. 4b presents the results for the gel obtained in phosphate buffer (pH 5.8, 10 mM)/DMSO (9/1 v/v) allowing a larger temperature range. The temperature was varied from 25 to 80 °C at a frequency of 1 Hz and 0.1% strain.

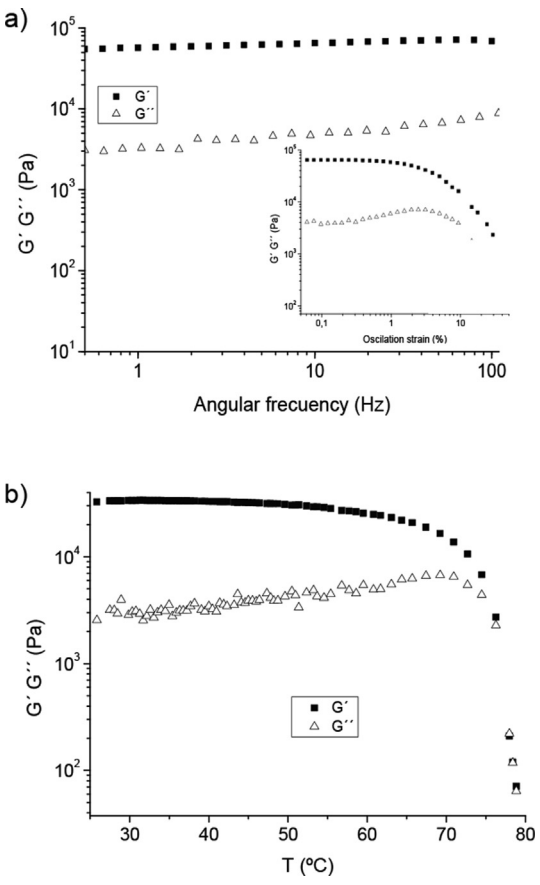

Fig. 4. Rheological measurements for the hydrogel from **2a** (5 mg mL^{-1}) in phosphate buffer (pH 5.8, 10 mM)/DMSO (9/1 v/v). a) Frequency sweeps with 0.1% strain and 1 Hz amplitude sweeps at 25 °C. b) Dependence of storage and loss modulus with the temperature using a heating rate of 0.1 °C /min and a constant frequency of 1 Hz and 0.1% strain.

The values for Ǵ decreased with the increase in temperature, allowing to determine a gelation temperature of 75 °C (transition temperature at which Ǵ is equal to Ǵ). A similar behavior was obtained for the organogel in glycerol, with the gelation temperature being 60 °C. It must be noted that the storage modulus started to decrease after 40 °C and the oscillation strain was maintained constant up to *ca.* 40 °C, increasing significantly after this temperature (ESI, Fig. S22).

3.5. Stimuli-***responsiveness***

Spectroscopic studies revealed the presence of dynamic equilibria in the hydrogels formed by **2a**. This opens the way to potential stimuli-responsive and self-healing behaviors. Thus, starting from the gel formed using 5 mg mL^{-1} of **2a** in H_2O/EtOH (9:1, v/v) the addition on the top of gel of 2 equiv. of NaOH from a 1 M solution, led to its gradual transformation into a fluid solution. Further addition of 2 equiv. of HCl from a 1 M solution led to the rapid conversion (<10 min) of this solution back into a stable gel (Fig. 5). This fully reversible gel-sol transition was observed for at least four cycles involving successive additions of equimolecular amounts of NaOH and HCl (ESI, Fig. S23).

As is common in gels, the reversible sol–gel transition for the hydrogels prepared from **2a** was also triggered by temperature and stable gels could be obtained after several cycles of heating above T_{gel} and further cooling. More remarkable was their responsiveness to ultrasounds that can allow for a self-healing behavior [68]. Thus, under sonication the gel changed into solution immediately with the gel reformed again in<10 min after suppression of this input.

3.6. Drug ***delivery*** *studies*

As mentioned above, the controlled delivery of active substances in the biomedical realm, represents one key application of hydrogels [16–24]. Such materials seem particularly well suited for transdermal drug delivery, for which the use of viscous matrices (i.e., ionic liquids or DESs) have been shown to provide interesting features [69–70]. In this regard, the potential of the hydrogel matrices based on **2a** for drug release was explored selecting (*S*)-Naproxen and caffeine as low molecular weight model drugs presenting very different chemical features (ESI, Fig. S24). While (*S*)-Naproxen is a carboxylic acid (hydrogen bond donor, HBD) with low solubility in water, caffeine presents some solubility in both water and alcohol, is weakly basic and contains several functional groups able to participate in supramolecular interactions as hydrogen bond acceptors (HBA). Moreover, both drugs are used in topical formulations [71–72]. The loaded hydrogel was prepared by mixing **2a** and the drug, dissolving the mixture in 0.2 mL of DMSO and adding then 1.8 mL of phosphate buffer (10 mM, pH = 5.8). The mixture was sonicated and left for 24 h to obtain a stable

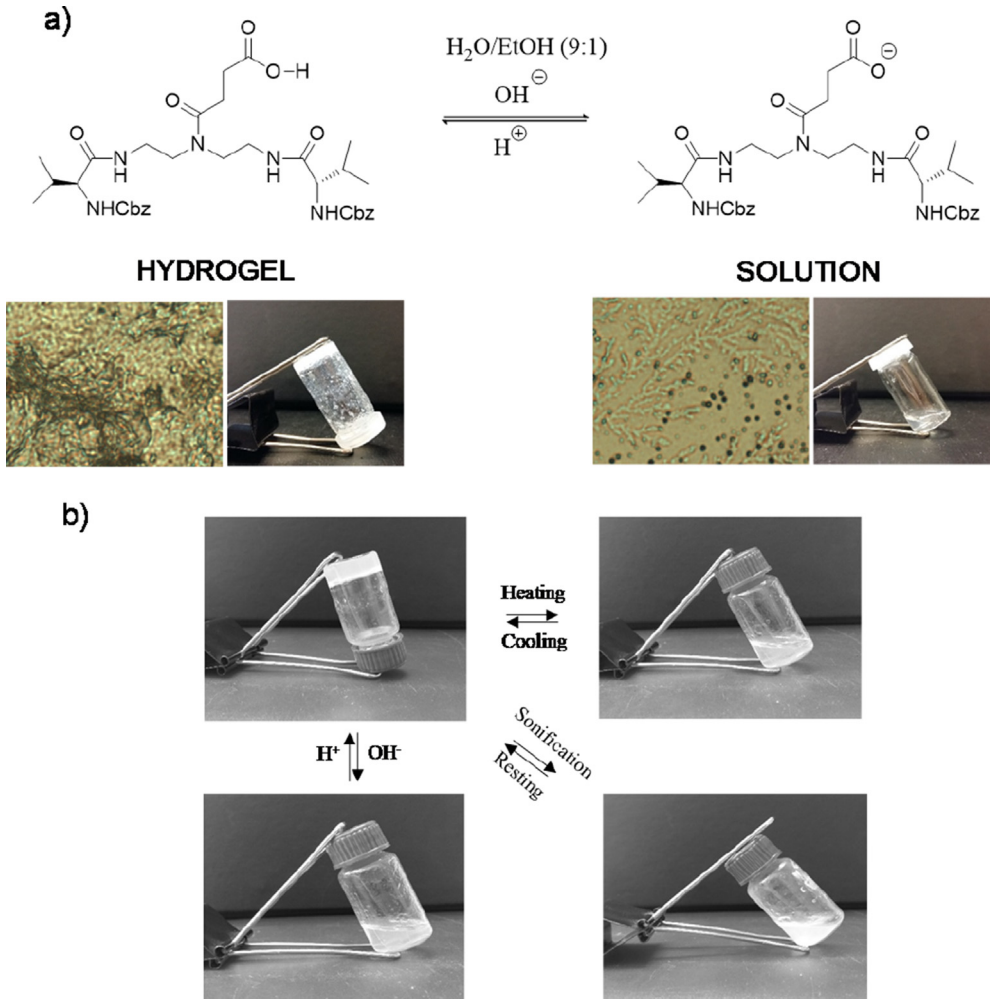

Fig. 5. a) Reversible pH-responsive gel-sol transition (**2a** 5 mg mL^{-1} in H_2O/EtOH (9:1 v/v)) and the corresponding optical microscopic morphology, b) Reversible sol-hydrogel transition triggered by temperature, pH and sonication.

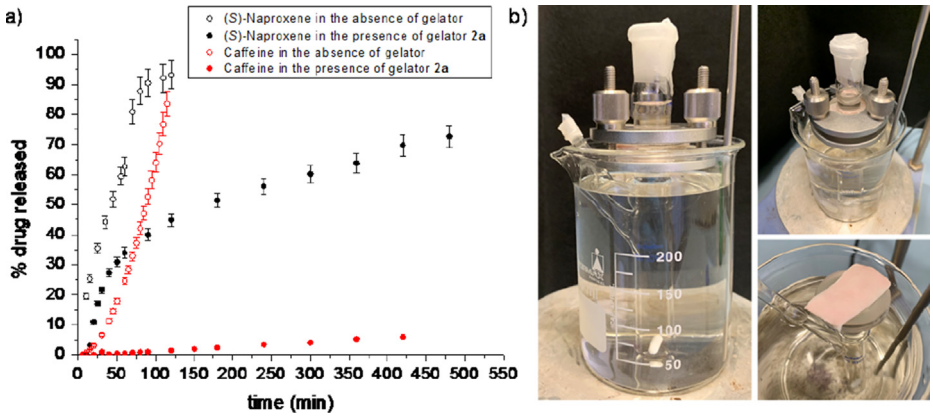

Fig. 6. a) Drug release profile in the absence and presence of gelator. Data points represent averages of two samples in the absence of LMWG and three samples in the presence of **2a**. b) Image of the Franz Cell and the pig skin membrane.

hydrogel containing 5 mg mL^{-1} of **2a** and 0.16 mg mL^{-1} of the active substance (*ca.* 0.4 mM for caffeine, for instance).

In vitro transdermal drug release studies were performed using a Franz diffusion Cell having a permeation orifice of 10 mm and a receiver chamber volume of 5 mL. A skin ear pig membrane of 1 mm thickness was used (Fig. 6b). This skin membrane was prepared following a protocol previously reported [73–74], then hydrated with miliQ® water and the receiver volume filled with

Table 3
Caffeine and (*S*)-Naproxen kinetic release parameters obtained by fitting to the different models selected using the hydrogel as the source[a].

Model	(*S*)-Naproxen[b]			Caffeine[c]		
	k (k_2)	n	r^2 (AICc)	k (k_2)	n	r^2 (AICc)
Zero-order	$13.78E^{-4} \pm 1.64E^{-4}$	1	0.813	$15.06E^{-5} \pm 0.23E^{-5}$	1	0.985
Higuchi	0.071 ± 0.012	0.5	−0.067	0.003 ± 0.001	0.5	−0.067
Alfrey	0.001 ± 1.701E-4 (0.01)	0.5	0.799	$15.06E^{-4} \pm 0.26E^{-5}$ (0.01)	0.5	0.945 (−17)
Peppas-Shalin	0.084 ± 0.015 (-0.001 ± 1.35E-3)	0.37 ± 0.07	0.963 (111)	$22.84E^{-3} \pm 2.46E^{-3}$ ($1.853E^{-4} \pm 4.238E^{-4}$)	0.49 ± 0.14	0.997 (42)
Ritger-Peppas	0.115 ± 0.021	0.3 ± 0.03	0.976 (107)	$1.494E^{-4} \pm 0.388E^{-4}$	1.01 ± 0.04	0.997 (−31)

[a]Hydrogel composition: Phosphate buffer (pH 5.8, 10 mM)/DMSO (9/1, v/v), k and k_2 represent kinetic constants and n is a diffusional exponent. [b] 0.31 mM. [c] 0.33 mM.

5 mL of a biocompatible phosphate buffer (10 mM, pH = 7.3). Drug release was monitored during *ca.* 24 h with the receptor compartment containing phosphate buffer (pH 7.3) immersed in a water bath at 35 ± 0.5 °C. Over this period, neither shrinkage, swelling or degradation of the gel was perceptible.

The release was analyzed in the receiving phase following the increase in the UV–visible absorption bands associated to the drugs (ESI, Fig. S25 and S26). For comparison, drug release profiles were also obtained for similar solutions of the drug, in the same solvent mixture, but in the absence of the LMWG **2a**. As shown in Fig. 6a, drug molecules were released from the hydrogel in a slow and continuous manner without any burst release up to 8 h. In the case of (*S*)-Naproxen, this release pattern was maintained after 24 h, although for caffeine an increased release was observe at this time, most likely associated to the partial loss observed for the properties of this gel (Fig. S27).

The presence of the hydrogel matrix significantly reduces the release of both drugs in comparison with the use of the similar solution as the source. This was particularly important in the case of caffeine. After the first hour, the release of (*S*)-Naproxen from the hydrogel was *ca.* half of that released from the solution and a similar ratio was observed after 2 h, while the release of caffeine from the hydrogel was about 20 times smaller than that from the solution, becoming *ca.* 40 times smaller when a period of 2 h was considered. The caffeine release from the solution was also slightly slower than that of (*S*)-Naproxen. When the drugs were entrapped in the hydrogel matrix the release after 8 h reached *ca.* 10% for caffeine and *ca.* 70 % for (*S*)-Naproxen. After 24 h, the drug content in both the gel and the membrane was also determined. The membrane was sonicated in the corresponding solution (phosphate buffer 10 mM pH = 8 for Naproxen and pH = 5.8 for caffeine) to determine the drug retained. In the presence of hydrogel, the drug retained inside the membrane was 23% and 13% for caffeine and (*S*)-Naproxen, and 31% and 0% the drug remained in the hydrogel respectively. The sum of the drug released, retained in the membrane and in the hydrogel matrix accounted for 94–95% of the total amount of drug used.

Different drug transport mechanisms have been reported and evaluated using the kinetics observed experimentally [75–78]. In the present case, the zero-order, Higuchi [79–81], Alfrey [82], Ritger-Peppas [83–86], and Peppas-Shalin [87–90] models were used after linearization to obtain additional information on the

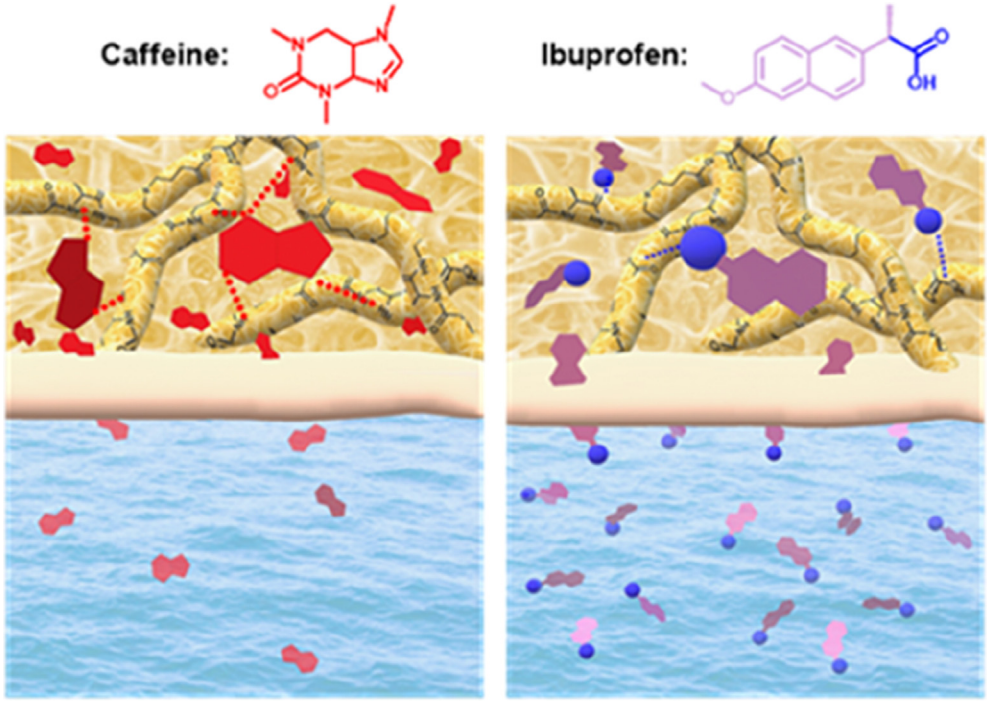

Fig. 7. Schematic representation of the differences in the controlled release of caffeine and ibuprofen.

mechanisms of drug release involved [91–92]. The r^2 and Akaike Information Criterion (AICc) [93–95] values were used as goodness of fit parameters as they are indicators of the model suitability for a given data set. From them, the Ritger-Peppas model provided the best fitting (Tables S3 and 4; ESI, Fig. S28).

Data in Table S3 indicate that the mechanism of (*S*)-Naproxen release from the phosphate buffer (pH 5.8, 10 mM)/DMSO (9/1, v/v) solution was controlled by both Fickian and non-Fickian diffusion (n = 0.66), whilst for caffeine the transport mechanism observed was anomalous (n = 1.88) In the case of the hydrogels, data in Table 3 show that the release was controlled by the Fickian diffusion (n = 0.3) for (*S*)-Naproxen and by an anomalous drug transport mechanism in the case of caffeine, leading to a zero-order release (n ≈ 1) [96–97].

Using a non-steady-state diffusion model, with the equation for the early-time being $M_t/M_o = 4(D_E{}^*(t\text{-}l)/h^2\,\pi)^{1/2}$ and the one for the late-time being $M_t/M_o = 1 - 8/\pi^2(\exp - \pi^2 D_L(t\text{-}l)/h^2)$, the relative diffusion coefficients of the drug molecules through the gel could be calculated [98–99]. Considering constant the amount of drug entrapped inside the membrane after a saturation period l (lag time 24 min and 21 min for caffeine and Naproxen respectively), the diffusion coefficient values determined were $D_E = 3.06\ 10^{-8}$ m^2/s (r^2 = 0.976) for (*S*)-Naproxen and $D_L = 1.64\ 10^{-10}$ m^2/s (r^2 = 0.908) for caffeine. Thus, caffeine was held more tightly by the gel resulting in their slower release [99]. This is likely to be due to the presence of electrostatic and hydrophilic interactions between the drug and gel matrix that will be particularly prevalent in the case of caffeine containing hydrogen bond acceptor functionalities complementary of the hydrogen bond donor sites in the molecule of the LMWG [100]. As schematically represented in Fig. 7, the higher basicity of caffeine allows developing a stronger network of hydrogen bonding interactions with the acidic fragments of the gelator, reducing the release rate. On the contrary, the weaker hydrogen bonding interactions of the acidic ibuprofen provide access to a faster release into the receiving phase. D values are comparable to those of small model drugs in other LMW gelling systems [97–98,101].

To analyze the contribution to the different release of both drugs from their interaction with the membrane, the drug flux at steady state (Jss, μg cm^2/h) across the membrane was calculated, in the absence of gelator, from the slope of the linear portion of the cumulative drug permeation through the membrane per unit of area versus time. The Jss values determined were 291 and 77 μg cm^2/h for (*S*)-Naproxen and caffeine respectively. This indicates that caffeine also interacts stronger with the membrane than (*S*)-Naproxen affording a reduced flux, although, according to the data presented in Fig. 7, the main factor affecting the slower release of caffeine must be associated to the supramolecular interactions between this drug and the hydrogel matrix.

4. Conclusion

In conclusion, a series of novel pseudopeptidic hydrogelators showing a rapid and reversible, ultrasound, pH and thermal responsiveness and displaying self-healing properties have been prepared and studied. Results demonstrate that an optimum lipophilicity of the amino acid residue is needed for an efficient gelation process. Thus, gelator **2a** was able to form stable gels in a wide range of solvents with a CGC value of 1 mg mL^{-1} in H_2O : EtOH (9:1, v/v), while compound **2c**, in which the aliphatic side chain was substituted by an aromatic one, was unable to form gels in any solvent studied at 5 mg mL^{-1}. An intermediate situation was found for **2b** differing from **2a** just by the presence of an additional methylene group in the side chain, forming much weaker gels than **2a**. The hydrogel formed by **2a** (0.5 mg mL^{-1}) in H_2O/EtOH (9:1, v/v) displayed thermal stability up to 60 °C while the hydrogel formed in H_2O/DMSO (9:1, v/v) was stable up to 70 °C. Stable hydrogels were also obtained in H_2O/EtOH (9:1, v/v) in the presence of a variety of buffers, including biologically relevant phosphate buffers, but were unstable in basic conditions. Preliminary drug delivery studies, using a Franz Diffusion Cell with a pig skin membrane, were carried out with caffeine and (*S*)-Naproxen as model drugs with very different features for supramolecular interactions. The results have revealed that the hydrogels allow for a continuous and significantly slower release of the drugs, which is particularly relevant for caffeine. The release process could be fitted to different mechanism models, with the best fitting achieved for the Ritger-Peppas model. The results from this model, in combination with the observation of quite different diffusion coefficients, drug fluxes at steady state and release rates, defined the presence of different drug release mechanisms for both drugs entrapped in the hydrogel matrix. The significantly slower release rate for caffeine when using the hydrogel as the source phase must be assigned to the higher complementarity, in terms of supramolecular interactions, between the drug and the LMWG, highlighting the potential of this complementarity as a design vector for the development of specific LMWGs for the focused and controlled release of active substances and drugs. Given the chemical structure of the LMWG in this work, the resulting hydrogels have both HBD and HBA capacities and, accordingly, provide potential for the interaction with a large variety of active substances, controlling their release. It must be noted that best properties are achieved under acidic pH, which can also define the range of drugs for application (stable and soluble under relatively acidic conditions). This also opens the way to control the release through small changes in pH. This is exemplified in the drug delivery studies carried out where the pH of the receiving phase was slightly different from the pH of the gel.

CRediT authorship contribution statement

Adriana Valls: Investigation, Writing – original draft. **M. Isabel Burguete:** Methodology, Supervision. **Laura Kuret:** Investigation. **Belén Altava:** Conceptualization, Methodology, Supervision, Writing – review & editing. **Santiago V. Luis:** Conceptualization, Methodology, Supervision, Writing – review & editing.

Declaration of Competing Interest

The authors declare that they have no known competing financial interests or personal relationships that could have appeared to influence the work reported in this paper.

Acknowledgements

This research was funded by FEDER/MINISTERIO DE CIENCIA, INNOVACIÓN Y UNIVERSIDADES, grant number RTI2018-098233-B-C22, Pla de Promoció de la Investigació de la Universitat Jaume I, grant UJI-B2019-40 and Consellería de Innovació, Universitat Ciencia de la Generalitat Valenciana (AICO/2021/139). A.V. work was funded by a MICINN predoctoral fellowship, grant FPU15/01191. Technical support from the SECIC of the UJI is acknowledged.

Appendix A. Supplementary material

Supplementary data to this article can be found online at https://doi.org/10.1016/j.molliq.2021.118051.

References

[1] D. Philp, J.F. Stoddart, Self-Assembly in Natural and Unnatural Systems, Angew. Chem. Int. Ed. Engl. 35 (11) (1996) 1154–1196, https://doi.org/10.1002/anie.199611541.

[2] M.B. Avinash, T. Govindaraju, Architectonics: Design of Molecular Architecture for Functional Applications, Acc. Chem. Res. 51 (2) (2018) 414–426, https://doi.org/10.1021/acs.accounts.7b00434.

[3] K. Deng, Z. Luo, L.i. Tan, Z. Quan, Self-assembly of anisotropic nanoparticles into functional superstructures, Chem. Soc. Rev. 49 (16) (2020) 6002–6038, https://doi.org/10.1039/D0CS00541J.

[4] A. Levin, T.A. Hakala, L. Schnaider, G.J.L. Bernardes, E. Gazit, T.P.J. Knowles, Biomimetic peptide self-assembly for functional materials, Nat. Rev. Chem. 4 (11) (2020) 615–634, https://doi.org/10.1038/s41570-020-0215-y.

[5] P. Dastidar, Supramolecular gelling agents: can they be designed?, Chem Soc. Rev. 37 (2008) 2699–2715, https://doi.org/10.1039/B807346E.

[6] L.E. Buerkle, S. Rowan, Supramolecular gels formed from multi-component low molecular weight species, J. Chem. Soc. Rev. 41 (2012) 6089–6102, https://doi.org/10.1039/C2CS35106D.

[7] E.R. Draper, D.J. Adams, How should multicomponent supramolecular gels be characterised?, Chem Soc. Rev. 47 (10) (2018) 3395–3405, https://doi.org/10.1039/C7CS00804J.

[8] P.R.A. Chivers, D.K. Smith, Shaping and structuring supramolecular gels, Nat. Rev. Mater. 4 (7) (2019) 463–478, https://doi.org/10.1038/s41578-019-0111-6.

[9] S.S. Babu, V.K. Praveen, A. Ajayaghosh, Functional π-Gelators and Their Applications, Chem. Rev. 114 (4) (2014) 1973–2129, https://doi.org/10.1021/cr400195e.

[10] F. Delbecq, R. Nguyen, E. Van Hecke, C. Len, Design and physicochemical properties of long and stiff fatty low molecular weight oleogelators, J. Mol. Liq. 295 (2019) 1111708, https://doi.org/10.1016/j.molliq.2019.111708.

[11] D.-X. Wang, M.-X. Wang, Exploring Anion−π Interactions and Their Applications in Supramolecular Chemistry, Acc. Chem. Res. 53 (7) (2020) 1364–1380, https://doi.org/10.1021/acs.accounts.0c00243.

[12] I.M. Stankovic, S.Q. Niu, M.B. Hall, S.O. Zaric, Role of aromatic amino acids in amyloid self-assembly, Int. J. Biol. Macromol. 156 (2020) 949–959, https://doi.org/10.1016/j.ijbiomac.2020.03.064.

[13] L.A. Estroff, A.D. Hamilton, Water Gelation by Small Organic Molecules, Chem. Rev. 104 (3) (2004) 1201–1218, https://doi.org/10.1021/cr0302049.

[14] V. Nele, J.P. Wojciechowski, J.P.K. Armstrong, M.M. Stevens, Tailoring Gelation Mechanisms for Advanced Hydrogel Applications, Adv. Funct. Mat. 30 (42) (2020) 2002759, https://doi.org/10.1002/adfm.202002759.

[15] J. Song, C. Michas, C.S. Chen, A.E. White, M.W. Grinstaff, From Simple to Architecturally Complex Hydrogel Scaffolds for Cell and Tissue Engineering Applications: Opportunities Presented by Two-Photon Polymerization, Adv. Healthcare Mater. 9 (1) (2020) 1901217, https://doi.org/10.1002/adhm.201901217.

[16] W. Cheng, Z. Ding, X. Zheng, Q. Lu, X. Kong, X. Zhou, G. Lu, D.L. Kaplan, Injectable hydrogel systems with multiple biophysical and biochemical cues for bone regeneration, Biomater. Sci. 8 (9) (2020) 2537–2548, https://doi.org/10.1039/D0BM00104J.

[17] A.S. Hoffman, Hydrogels for biomedical applications, Adv. Drug Delivery Rev. 64 (2012) 18–23, https://doi.org/10.1016/j.addr.2012.09.010.

[18] Z. Li, J. Huang, J. Wu, pH-Sensitive nanogels for drug delivery in cancer therapy, Biomater. Sci. 9 (3) (2021) 574–589, https://doi.org/10.1039/D0BM01729A.

[19] J. Mayr, C. Saldías, D. Díaz Díaz, Release of small bioactive molecules from physical gels, Chem. Soc. Rev. 47 (4) (2018) 1484–1515, https://doi.org/10.1039/C7CS00515F.

[20] Y. Guo, J. Bae, Z. Fang, P. Li, F. Zhao, G. Yu, Hydrogels and Hydrogel-Derived Materials for Energy and Water Sustainability, Chem. Rev. 120 (15) (2020) 7642–7707, https://doi.org/10.1021/acs.chemrev.0c00345.

[21] M.D. Segarra-Maset, V.J. Nebot, J.F. Miravet, B. Escuder, Control of molecular gelation by chemical stimuli, Chem. Soc. Rev. 42 (17) (2013) 7086–7098, https://doi.org/10.1039/C2CS35436E.

[22] C.D. Jones, J.W. Steed, Gels with sense: supramolecular materials that respond to heat, light and sound, Chem. Soc. Rev. 45 (23) (2016) 6546–6596, https://doi.org/10.1039/C6CS00435K.

[23] N. Falcone, H.-B. Kraatz, Supramolecular Assembly of Peptide and Metallopeptide Gelators and Their Stimuli-Responsive Properties in Biomedical Applications, Chem. Eur. J. 24 (54) (2018) 14316–14328, https://doi.org/10.1002/chem.201801247.

[24] M. Kuddushi, J. Mata, N. Malek, Self-Sustainable, self-healable, Load Bearable and Moldable stimuli responsive ionogel for the Selective Removal of Anionic Dyes from aqueous medium, J. Mol. Liq. 298 (2020) 112048, https://doi.org/10.1016/j.molliq.2019.112048.

[25] F. Raza, Y. Zhu, L.i. Chen, X. You, J. Zhang, A. Khan, M.W. Khan, M. Hasnat, H. Zafar, J. Wu, L. Ge, Paclitaxel-loaded pH responsive hydrogel based on self-assembled peptides for tumor targeting, Biomater. Sci. 7 (5) (2019) 2023–2036, https://doi.org/10.1039/C9BM00139E.

[26] F.-D. Meng, Y.-X. Ni, S.-F. Ji, X.-H. Fu, Y.-H. Wei, J. Sun, Z.-b. Li, Dual thermal- and pH-responsive polypeptide-based hydrogels, Chin. J. Polym. Sci. 35 (10) (2017) 1243–1252, https://doi.org/10.1007/s10118-017-1959-9.

[27] H. Shaikh, J.Y. Rho, L.J. Macdougall, P. Gurnani, A.M. Lunn, J. Yang, S. Huband, E.D.H. Mansfield, R. Peltier, S. Perrier, Hydrogel and Organogel Formation by Hierarchical Self-Assembly of Cyclic Peptides Nanotubes, Chem. Eur. J. 24 (71) (2018) 19066–19074, https://doi.org/10.1002/chem.201804576.

[28] C. Wang, Q. Chen, F. Sun, D. Zhang, G. Zhang, Y. Huang, R. Zhao, D. Zhu, Multistimuli Responsive Organogels Based on a New Gelator Featuring Tetrathiafulvalene and Azobenzene Groups: Reversible Tuning of the Gel−Sol Transition by Redox Reactions and Light Irradiation, J. Am. Chem. Soc. 132 (9) (2010) 3092–3096, https://doi.org/10.1021/ja910721s.

[29] W. Cao, X. Zhang, X. Miao, Z. Yang, H. Xu, γ-Ray-responsive supramolecular hydrogel based on a diselenide-containing polymer and a peptide, Angew. Chem. Int. Ed. 52 (24) (2013) 6233–6237, https://doi.org/10.1002/anie.201300662.

[30] C.-W. Chu, L. Stricker, T.M. Kirse, M. Hayduk, B.J. Ravoo, Light-Responsive Arylazopyrazole Gelators: From Organic to Aqueous Media and from Supramolecular to Dynamic Covalent Chemistry, Chem. Eur. J. 25 (24) (2019) 6131–6140, https://doi.org/10.1002/chem.201806042.

[31] Y. Gao, Y.i. Kuang, Z.-F. Guo, Z. Guo, I.J. Krauss, B. Xu, Enzyme-Instructed Molecular Self-assembly Confers Nanofibers and a Supramolecular Hydrogel of Taxol Derivative, J. Am. Chem. Soc. 131 (38) (2009) 13576–13577, https://doi.org/10.1021/ja904411z.

[32] N. Mehwish, X. Dou, Y. Zhao, C.-L. Feng, Supramolecular fluorescent hydrogelators as bio-imaging probes, Mater. Horizons. 6 (1) (2019) 14–44, https://doi.org/10.1039/C8MH01130C.

[33] C.A. DeForest, K.S. Anseth, Cytocompatible click-based hydrogels with dynamically tunable properties through orthogonal photoconjugation and photocleavage reactions, Nat. Chem. 3 (12) (2011) 925–931, https://doi.org/10.1038/nchem.1174.

[34] J. Boekhoven, M. Koot, T.A. Wezendonk, R. Eelkema, J.H. van Esch, A Self-Assembled Delivery Platform with Post-production Tunable Release Rate, J. Am. Chem. Soc. 134 (31) (2012) 12908–12911, https://doi.org/10.1021/ja3051876.

[35] S.A. Elkassih, P. Kos, H.u. Xiong, D.J. Siegwart, Degradable redox-responsive disulfide-based nanogel drug carriers via dithiol oxidation polymerization, Biomater. Sci. 7 (2) (2019) 607–617, https://doi.org/10.1039/C8BM01120F.

[36] Y. Cheng, C. He, J. Ding, C. Xiao, X. Zhuang, X. Chen, Thermosensitive hydrogels based on polypeptides for localized and sustained delivery of anticancer drugs, Biomaterials 34 (38) (2013) 10338–10347, https://doi.org/10.1016/j.biomaterials.2013.09.064.

[37] M.C. Giano, Z. Ibrahim, S.H. Medina, K.A. Sarhane, J.M. Christensen, Y. Yamada, G. Brandacher, J.P. Schneider, Injectable bioadhesive hydrogels with innate antibacterial properties, Nat. Commun. 5 (2014) 4095, https://doi.org/10.1038/ncomms5095.

[38] M.A. Anderson, J.E. Burda, Y. Ren, Y. Ao, T.M. O'Shea, R. Kawaguchi, G. Coppola, B.S. Khakh, T.J. Deming, M.V. Sofroniew, Astrocyte scar formation aids central nervous system axon regeneration, Nature 532 (7598) (2016) 195–200, https://doi.org/10.1038/nature17623.

[39] Y. Zhao, Z. Cui, B. Liu, J. Xiang, D. Qiu, Y. Tian, X. Qu, Z. Yang, An Injectable Strong Hydrogel for Bone Reconstruction, Adv. Healthcare Mater. 8 (17) (2019) 1900709, https://doi.org/10.1002/adhm.201900709.

[40] S.M. Carvalho, A.A.P. Mansur, N.S.V. Capanema, I.C. Carvalho, P. Chagas, L.C.A. de Oliveira, H.S. Mansur, Synthesis and in vitro assessment of anticancer hydrogels composed by carboxymethylcellulose-doxorubicin as potential transdermal delivery systems for treatment of skin cancer, J. Mol. Liq. 266 (2018) 425–440, https://doi.org/10.1016/j.molliq.2018.06.085.

[41] S. Fleming, R.V. Ulijn, Design of nanostructures based on aromatic peptide amphiphiles, Chem. Soc. Rev. 43 (23) (2014) 8150–8177, https://doi.org/10.1039/C4CS00247D.

[42] X.-Q. Dou, C.-L. Feng, Amino Acids and Peptide-Based Supramolecular Hydrogels for Three-Dimensional Cell Culture, Adv. Mater. 29 (16) (2017) 1604062, https://doi.org/10.1002/adma.201604062.

[43] S.M. Ramalhete, K.P. Nartowski, N. Sarathchandra, J.S. Foster, A.N. Round, J. Angulo, G.O. Lloyd, Y.Z. Khimyak, Supramolecular Amino Acid Based Hydrogels: Probing the Contribution of Additive Molecules using NMR Spectroscopy, Chem. Eur. J. 23 (33) (2017) 8014–8024, https://doi.org/10.1002/chem.201700793.

[44] T. Das, M. Häring, D. Haldar, D. Díaz Díaz, Phenylalanine and derivatives as versatile low-molecular-weight gelators: design, structure and tailored function, Biomater. Sci. 6 (2018) 38–59, https://doi.org/10.1039/c7bm00882a.

[45] S.V. Luis, I. Alfonso, Bioinspired Chemistry Based on Minimalistic Pseudopeptides, Acc. Chem. Res. 47 (1) (2014) 112–124, https://doi.org/10.1021/ar400085p.

[46] Emily R. Draper, Kyle L. Morris, Marc A. Little, Jaclyn Raeburn, Catherine Colquhoun, Emily R. Cross, Tom.O. McDonald, Louise C. Serpell, Dave J. Adams, Hydrogels formed from Fmoc amino acids, CrystEngComm. 17 (42) (2015) 8047–8057, https://doi.org/10.1039/C5CE00801H.

[47] Y.L. Milli, N. Zanna, A. Merlettini, M.D. Giosia, M. Calvaresi, M.L. Focarete, C. Tomasini, Pseudopeptide-Based Hydrogels Trapping Methylene Blue and Eosin Y, Chem-Eur. J. 22 (2016) 12106–12112, https://doi.org/10.1002/chem.201601861.

[48] Annada Rajbhandary, Danielle M. Raymond, Bradley L. Nilsson, Self-Assembly, Hydrogelation, and Nanotube Formation by CationModified Phenylalanine Derivatives, Langmuir 33 (23) (2017) 5803–5813, https://doi.org/10.1021/acs.langmuir.7b00686.

[49] Nicola Zanna, Andrea Merlettini, Claudia Tomasini, Self-healing hydrogels triggered by amino acids, Org. Chem. Front. 3 (12) (2016) 1699–1704, https://doi.org/10.1039/C6QO00476H.

[50] J.W. Steed, Anion-tuned supramolecular gels: a natural evolution from urea supramolecular chemistry, Chem. Soc. Rev. 39 (2010) 3686–3699, https://doi.org/10.1039/B926219A.
[51] Adriana Valls, Adrián Castillo, Raúl Porcar, Sami Hietala, Belén Altava, Eduardo García-Verdugo, Santiago V. Luis, Urea-Based Low-Molecular-Weight Pseudopeptidic Organogelators for the Encapsulation and Slow Release of (R)–Limonene, J. Agric. Food Chem. 68 (26) (2020) 7051–7061, https://doi.org/10.1021/acs.jafc.0c01184.
[52] J. Rubio, I. Alfonso, M.I. Burguete, S.V. Luis, Interplay between hydrophilic and hydrophobic interactions in the self-assembly of a gemini amphiphilic pseudopeptide: from nano-spheres to hydrogels, Chem. Commun. 48 (2012) 2210–2212, https://doi.org/10.1039/C2CC17153H.
[53] P.D. Wadhavane, L. Gorla, A. Ferrer, B. Altava, M.I. Burguete, M.A. Izquierdo, S. V. Luis, Coordination behaviour of new open chain and macrocyclic peptidomimetic compounds with copper(II), RSC Adv. 25 (2015) 72579–72589, https://doi.org/10.1039/c5ra15852d.
[54] M.Isabel Burguete, Jean M.J. Fréchet, Eduardo García-Verdugo, Miroslav Janco, Santiago V. Luis, Frantisek Svec, María J. Vicent, Mingcheng Xu, New CSPs based on peptidomimetics: efficient chiral selectors in enantioselective separations, Polym. Bull. 48 (1) (2002) 9–15, https://doi.org/10.1007/s00289-002-0005-3.
[55] Lingaraju Gorla, Vicente Martí-Centelles, Belén Altava, M.Isabel Burguete, Santiago V. Luis, The role of the side chain in the conformational and self-assembly patterns of C2-symmetric Val and Phe pseudopeptidic derivatives, CrystEngComm 21 (14) (2019) 2398–2408, https://doi.org/10.1039/C8CE02088D.
[56] R.G. Weiss, P. Terech (Eds.), Molecular Gels: Materials with Self-Assembled Fibrillar Networks, Springer, 2005.
[57] Ron Orbach, Iris Mironi-Harpaz, Lihi Adler-Abramovich, Estelle Mossou, Edward P. Mitchell, V.Trevor Forsyth, Ehud Gazit, Dror Seliktar, The rheological and structural properties of Fmoc-peptide-based hydrogels: the effect of aromatic molecular architecture on self-assembly and physical characteristics, Langmuir 28 (4) (2012) 2015–2022, https://doi.org/10.1021/la204426q.
[58] Masahiro Suzuki, Teruaki Sato, Akio Kurose, Hirofusa Shirai, Kenji Hanabusa, New low-molecular weight gelators based on L-valine and L-isoleucine with various terminal groups, Tetrahedron Lett. 46 (16) (2005) 2741–2745, https://doi.org/10.1016/j.tetlet.2005.02.144.
[59] A. Shome, S. Debnath, P.K. Das, Head Group Modulated pH-Responsive Hydrogel of Amino Acid-Based Amphiphiles: Entrapment and Release of Cytochrome c and Vitamin B12, Langmuir 24 (2008) 4280–4288, https://doi.org/10.1021/la704024p.
[60] Ahmed H. Lotfallah, M.Isabel Burguete, Ignacio Alfonso, Santiago V. Luis, Highly stable oil-in-water emulsions with a gemini amphiphilic pseudopeptide, RSC Adv. 5 (46) (2015) 36890–36893, https://doi.org/10.1039/C5RA05121E.
[61] Jos M Poolman, Job Boekhoven, Anneke Besselink, Alexandre G.L Olive, Jan H van Esch, Rienk Eelkema, Variable gelation time and stiffness of low-molecular-weight hydrogels through catalytic control over self-assembly, Nat. Protoc. 9 (4) (2014) 977–988, https://doi.org/10.1038/nprot.2014.055.
[62] A.R. Meyer, C.R. Bender, D.M. dos Santos, F.I. Ziembowicz, C.P. Frizzo, M.A. Villetti, J.M. Reichert, N. Zanatta, H.G. Bonacorso, M.A.P. Martins, Effect of slight structural changes on the gelation properties of *N*-phenylstearamide supramolecular gels, Soft Matter 14 (2018) 6716–6727, https://doi.org/10.1039/C8SM00961A.
[63] A.D. Schlüter, J.P. Rabe, Dendronized Polymers: Synthesis, Characterization, Assembly at Interfaces, and Manipulation, Angew. Chem. Int. Ed 39 (2000) 864–883, https://doi.org/10.1002/(sici)1521-3773(20000303)39:5<864::aid-anie864>3.0.co;2-e.
[64] Didier Astruc, Elodie Boisselier, Cátia Ornelas, Dendrimers designed for functions: from physical, photophysical, and supramolecular properties to applications in sensing, catalysis, molecular electronics, photonics, and nanomedicine Chem, Rev. 110 (4) (2010) 1857–1959, https://doi.org/10.1021/cr900327d.
[65] D.C. Lee, D. Chapman, Infrared spectroscopic studies of biomembranes and model membranes, Bioscience Rep. 6 (1986) 235–256, https://doi.org/10.1007/BF01115153.
[66] V.L Furer, Calculation of the IR spectra of toluene-2,4-bis (methyl) carbamate, J. Mol. Struct. 476 (1-3) (1999) 215–222, https://doi.org/10.1016/S0022-2860(98)00549-3.
[67] C. Yan, D. Pochan, Rheological properties of peptide-based hydrogels for biomedical and other applications, Chem. Soc. Rev. 39 (2010) 3528–3540, https://doi.org/10.1039/b919449p.
[68] X. Yu, L. Chen, M. Zhang, T. Yi, Low-molecular-mass gels responding to ultrasound and mechanical stress: towards self-healing materials, Chem. Soc. Rev. 43 (2014) 5346–5371, https://doi.org/10.1039/C4CS00066H.
[69] Eden E.L. Tanner, Alexander M. Curreri, Joel P.R. Balkaran, Nadia C. Selig-Wober, Andrew B. Yang, Carter Kendig, Matthias P. Fluhr, Nicole Kim, Samir Mitragotri, Design Principles of Ionic Liquids for Transdermal Drug Delivery, Adv. Mat. 31 (27) (2019) 1901103, https://doi.org/10.1002/adma.201901103.
[70] Qin M. Qi, Miya Duffy, Alex M. Curreri, Joel P.R. Balkaran, Eden E.L. Tanner, Samir Mitragotri, Comparison of Ionic Liquids and Chemical Permeation Enhancers for Transdermal Drug Delivery, Adv. Funct. Mat. 30 (45) (2020) 2004257, https://doi.org/10.1002/adfm.202004257.
[71] Francisca Rodrigues, Ana Catarina Alves, Claudia Nunes, Bruno Sarmento, M. Helena Amaral, Salette Reis, M.Beatriz P.P. Oliveira, Permeation of topically applied caffeine from a food by—product in cosmetic formulations: Is nanoscale in vitro approach an option?, Int J. Pharm. 513 (1-2) (2016) 496–503, https://doi.org/10.1016/j.ijpharm.2016.09.059.
[72] Jan H. Vaile, Paul Davis, Topical NSAIDs for Musculoskeletal Conditions, Drugs 56 (5) (1998) 783–799, https://doi.org/10.2165/00003495-199856050-00004.
[73] Pankaj Karande, Amit Jain, Samir Mitragotri, Relationships between skin's electrical impedance and permeability in the presence of chemical enhancers, J. Control. Release 110 (2) (2006) 307–313, https://doi.org/10.1016/j.jconrel.2005.10.012.
[74] M.-A. Bolzinger, S. Briançon, J. Pelletier, H. Fessi, Y. Chevalier, Percutaneous release of caffeine from microemulsion, emulsion and gel dosage forms, Eur. J. Pharm. Biopharm. 68 (2) (2008) 446–451, https://doi.org/10.1016/j.ejpb.2007.10.018.
[75] Laura Serra, Joseph Doménech, Nicholas A. Peppas, Drug transport mechanisms and release kinetics from molecularly designed poly(acrylic acid-g-ethylene glycol) hydrogels, Biomaterials 27 (31) (2006) 5440–5451, https://doi.org/10.1016/j.biomaterials.2006.06.011.
[76] M. L, Bruschi in Strategies to Modify the Drug Release from Pharmaceutical Systems, Elsevier (2015) 37–62.
[77] Shahid Nawaz, Samiullah Khan, Umar Farooq, Malik Salman Haider, Nazar Muhammad Ranjha, Akhtar Rasul, Ahmad Nawaz, Numera Arshad, Rabia Hameed, Biocompatible hydrogels for the controlled delivery of anti-hypertensive agent: development, characterization and in vitro evaluation, Des. Monomers Polym. 21 (1) (2018) 18–32, https://doi.org/10.1080/15685551.2018.1445416.
[78] Paul Wan Sia Heng, Lai Wah Chan, Michael G Easterbrook, Xiaoman Li, Investigation of the influence of mean HPMC particle size and number of polymer particles on the release of aspirin from swellable hydrophilic matrix tablets, J. Control. Release 76 (1-2) (2001) 39–49, https://doi.org/10.1016/S0168-3659(01)00410-2.
[79] Takeru Higuchi, Rate of Release of Medicaments from Ointment Bases Containing Drugs in Suspension, J. Pharm. Sci. 50 (10) (1961) 874–875, https://doi.org/10.1002/jps.2600501018.
[80] T. Higuchi, Mechanism of sustained-action medication. Theoretical analysis of rate of release of solid drugs dispersed in solid matrices, J. Pharm. Sci. 52 (12) (1963) 1145–1149, https://doi.org/10.1002/jps.2600521210.
[81] P. Gao, P.R. Nixon, J.W. Skoug, Diffusion in HPMC Gels. II. Prediction of Drug Release Rates from Hydrophilic Matrix Extended-Release Dosage Forms, Pharm. Res. 12 (1995) 965–971, https://doi.org/10.1023/A:1016246028338.
[82] Turner Alfrey, E.F. Gurnee, W.G. Lloyd, Diffusion in glassy polymers, J. Polym. Sci. C. Polym. Symp. 12 (1) (1966) 249–261, https://doi.org/10.1002/polc.5070120119.
[83] Richard W. Korsmeyer, Nikolaos A. Peppas, Solute and penetrant diffusion in swellable polymers. III. Drug release from glassy poly(HEMA-co-NVP) copolymers, J. Control. Release 1 1 (2) (1984) 89–98, https://doi.org/10.1016/0168-3659(84)90001-4.
[84] Philip L. Ritger, Nikolaos A. Peppas, A simple equation for description of solute release I. Fickian and non-fickian release from non-swellable devices in the form of slabs, spheres, cylinders or discs, J. Control. Release 5 (1) (1987) 23–36, https://doi.org/10.1016/0168-3659(87)90034-4.
[85] Balaji Narasimhan, Nikolaos A. Peppas, Molecular Analysis of Drug Delivery Systems Controlled by Dissolution of the Polymer Carrier, J. Pharm. Sci. 86 (3) (1997) 297–304, https://doi.org/10.1021/js960372z.
[86] Nikolaos A. Peppas, Jennifer J. Sahlin, A simple equation for the description of solute release. III. Coupling of diffusion and relaxation, Int. J. Pharm. 57 (2) (1989) 169–172, https://doi.org/10.1016/0378-5173(89)90306-2.
[87] R.W. Korsmeyer, S.R. Lustig, N.A. Peppas, Solute and penetrant diffusion in swellable polymers. I. Mathematical modeling, J. Polym. Sci. B Polym. Phys. 24 (1986) 395–408, https://doi.org/10.1002/polb.1986.090240214.
[88] R.W. Korsmeyer, E. Von Meerwall, N.A. Peppas, Solute and penetrant diffusion in swellable polymers. II. Verification of theoretical models, J. Polym. Sci. B Polym. Phys. 24 (1986) 409–434, https://doi.org/10.1002/polb.1986.090240215.
[89] S.R. Lustig, N.A. Peppas, Solute and penetrant diffusion in swellable polymers. VII. A free volume-based model with mechanical relaxation, J. Appl. Polym. Sci. 33 (1987) 533–549, https://doi.org/10.1002/app.1987.070330221.
[90] N. A. Peppas, R. W. Korsmeyer, Dynamically swelling hydrogels in controlled release applications in Hydrogels in Medicine and Pharmacy, Vol. 3 Properties and Applications; (Ed. N. A. Peppas) CRC Press: Boca Raton, (1987) 109–136.
[91] James E. Polli, G.Singh Rekhi, Larry L. Augsburger, Vinod P. Shah, Methods to Compare Dissolution Profiles and a Rationale for Wide Dissolution Specifications for Metoprolol Tartrate tablets, J. Pharm. Sci. 86 (6) (1997) 690–700, https://doi.org/10.1021/js960473x.
[92] Paulo Costa, José Manuel Sousa Lobo, Modeling and comparison of dissolution profiles, Eur. J. Pharm. Sci. 13 (2) (2001) 123–133, https://doi.org/10.1016/S0928-0987(01)00095-1.
[93] J. Singh, S. Gupta, H. Kaur, Prediction of in vitro Drug Release Mechanisms from Extended Release Matrix Tablets using SSR/R^2 Technique, Trends, Appl. Sci. Res. 6 (2011) 400–409, https://doi.org/10.3923/tasr.2011.400.409.
[94] Kiyoshi Yamaoka, Terumichi Nakagawa, Toyozo Uno, Application of Akaike's information criterion (AIC) in the evaluation of linear pharmacokinetic equations, J. Pharmacokinet. Biopharm. 6 (2) (1978) 165–175, https://doi.org/10.1007/BF01117450.
[95] Peter Kletting, Gerhard Glatting, Model selection for time-activity curves: The corrected Akaike information criterion and the F-test, Z. Med. Phys. 19 (3) (2009) 200–206, https://doi.org/10.1016/j.zemedi.2009.05.003.

[96] J. Li, D.J. Mooney, Designing hydrogels for controlled drug delivery, Nat. Rev. Mater. 1 (2016) 16071, https://doi.org/10.1038/natrevmats.2016.71.
[97] David Díaz Díaz, Emmanuelle Morin, Eva M. Schön, Ghyslain Budin, Alain Wagner, Jean-Serge Remy, Tailoring drug release profile of low-molecular-weight hydrogels by supramolecular co-assembly and thiol–ene orthogonal coupling, J. Mat. Chem. 21 (3) (2011) 641–644, https://doi.org/10.1039/C0JM03399E.
[98] C.K. Thota, N. Yadav, V.S. Chauhan, A novel highly stable and injectable hydrogel based on a conformationally restricted ultrashort peptide, Sci. Rep. 6 (2016) 31167, https://doi.org/10.1038/srep31167.
[99] Jiban J. Panda, Aseem Mishra, Atanu Basu, Virander S. Chauhan, Stimuli Responsive Self-Assembled Hydrogel of a Low Molecular Weight Free Dipeptide with Potential for Tunable Drug Delivery, Biomacromolecules 9 (8) (2008) 2244–2250, https://doi.org/10.1021/bm800404z.
[100] Arianna Friggeri, Ben L Feringa, Jan van Esch, Entrapment and release of quinoline derivatives using ahydrogel of a low molecular weight gelator, J. Control. Release 97 (2) (2004) 241–248, https://doi.org/10.1016/j.jconrel.2004.03.012.
[101] M.C. Branco, D.J. Pochan, N.J. Wagner, J.P. Schneider, Macromolecular diffusion and release from self-assembled b-hairpin peptide hydrogels, Biomaterials 30 (2009) 1339–1347, https://doi.org/10.1016/j.biomaterials.2008.11.019.